Florida International University

FIU Digital Commons

Electrical and Computer Engineering Faculty Publications

College of Engineering and Computing

12-1-2007

A uniform geometrical theory of diffraction for predicting fields of sources near or on thin planar positive/negative material discontinuities

T. Lertwiriyaprapa
The Ohio State University

P. H. Pathak
The Ohio State University

J. L. Volakis
The Ohio State University

Follow this and additional works at: https://digitalcommons.fiu.edu/ece_fac

Recommended Citation

Lertwiriyaprapa, T.; Pathak, P. H.; and Volakis, J. L., "A uniform geometrical theory of diffraction for predicting fields of sources near or on thin planar positive/negative material discontinuities" (2007). *Electrical and Computer Engineering Faculty Publications*. 72.
https://digitalcommons.fiu.edu/ece_fac/72

This work is brought to you for free and open access by the College of Engineering and Computing at FIU Digital Commons. It has been accepted for inclusion in Electrical and Computer Engineering Faculty Publications by an authorized administrator of FIU Digital Commons. For more information, please contact dcc@fiu.edu.

A Uniform Geometrical Theory of Diffraction for predicting fields of sources near or on thin planar positive/negative material discontinuities

T. Lertwiriyaprapa,[1] P. H. Pathak,[1] and J. L. Volakis[1]

Received 7 May 2007; revised 19 August 2007; accepted 30 August 2007; published 13 December 2007.

[1] Relatively simple and accurate closed form Uniform Geometrical Theory of Diffraction (UTD) solutions are obtained for describing the radiated and surface wave fields, respectively, which are excited by sources near or on thin, planar, canonical two-dimensional (2-D) double positive/double negative (DPS/DNG) material discontinuities. Unlike most previous works, which analyze the plane wave scattering by such DPS structures via the Wiener-Hopf (W-H) or Maliuzhinets methods, the present development can also treat problems of the radiation by and coupling between antennas near or on finite material coatings on large metallic platforms. The latter is made possible mainly through the introduction of important higher-order UTD slope diffraction terms which are developed here in addition to first-order UTD. The present solutions are simpler to use because, in part, they do not contain the complicated split functions of the W-H solutions nor the complex Maliuzhinets functions. Unlike the latter methods based on approximate boundary conditions, the present solutions, which are developed via a heuristic spectral synthesis approach, recover the proper local plane wave Fresnel reflection and transmission coefficients and surface wave constants of the DPS/DNG material. They also include the presence of backward surface waves in DNG media. Besides being asymptotic solutions of the wave equation, the present UTD diffracted fields satisfy reciprocity, the radiation condition, boundary conditions on the conductor, and the Karp-Karal lemma which dictates that the first-order UTD space waves vanish on a material interface.

Citation: Lertwiriyaprapa, T., P. H. Pathak, and J. L. Volakis (2007), A Uniform Geometrical Theory of Diffraction for predicting fields of sources near or on thin planar positive/negative material discontinuities, *Radio Sci.*, *42*, RS6S18, doi:10.1029/2007RS003689.

1. Introduction

[2] Relatively simple and accurate closed form expressions are obtained, in the format of the asymptotic high frequency UTD ray method [*Kouyoumjian and Pathak*, 1974; *Pathak*, 1992], for describing the first-order diffraction, as well as slope diffraction, by discontinuities in thin, planar 2-D, canonical, isotropic and homogeneous DPS/DNG material configurations which are excited by a line (or line dipole) source. As is commonly classified, DPS materials are those which exhibit positive values of electrical permittivity and permeability while DNG materials are supposed to exhibit negative values for these quantities [*Engheta and Ziolkowski*, 2005]. Actually the UTD solutions obtained here also remain valid if one of these electrical parameters of the material is positive, while the other is negative. The source can be placed nearby or directly on, or even be embedded in the material; furthermore the source can also be allowed to recede far away from the surface. These UTD solutions would be useful for predicting the behavior of the fields radiated by antennas far from, near, or on metallic structures with a finite size material coating, and for predicting the coupling between such antennas. The specific canonical configurations of interest are shown in Figures 1 and 2. In particular, Figure 1a illustrates the diffraction from the junction between two thin, planar DPS/DNG grounded material slabs of different thickness

[1]ElectroScience Laboratory, Department of Electrical and Computer Engineering, Ohio State University, Columbus, Ohio, USA.

Copyright 2007 by the American Geophysical Union.
0048-6604/07/2007RS003689

1944799x, 2007, 6, Downloaded from https://agupubs.onlinelibrary.wiley.com/doi/10.1029/2007RS003689, Wiley Online Library on [23/02/2023]. See the Terms and Conditions (https://onlinelibrary.wiley.com/terms-and-conditions) on Wiley Online Library for rules of use; OA articles are governed by the applicable Creative Commons License

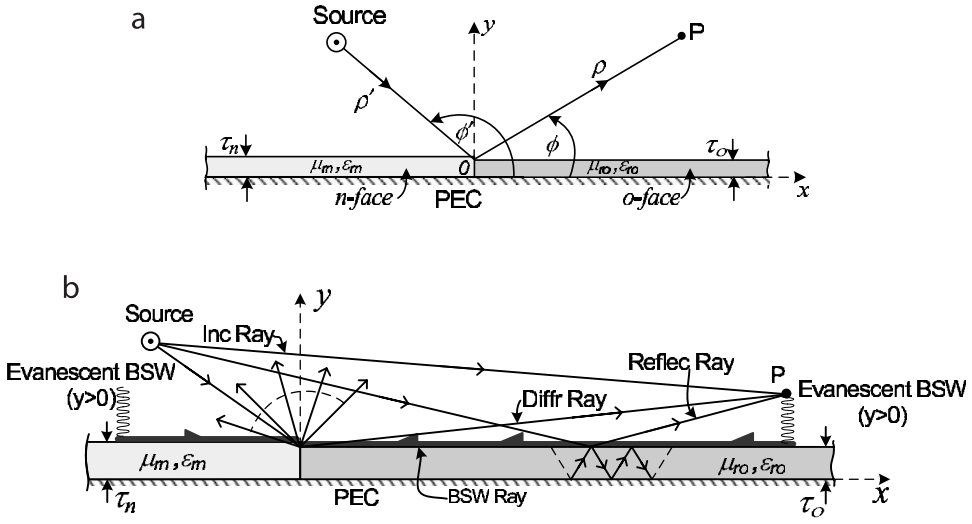

Figure 1. Junction between two different, thin, planar DPS/DNG material slabs on a perfect electric conductor (PEC) ground plane with a line source excitation. (a) A line source excitation. (b) Ray mechanisms.

and different electrical properties. Also Figure 2a illustrates the problem of wave diffraction by a thin, DPS/DNG material half plane. The configurations in Figures 1 and 2 are surrounded by free space. The material thickness is assumed to be a small fraction (e.g., one tenth) of the free space wavelength. The uniform line source or line dipole source can be either of the electric or magnetic type. Unfortunately, exact analytical solutions to the above problems of discontinuities in diffraction by material coated metallic surfaces are not currently available in a form suitable and tractable for engineering applications. Also it is noted that conventional numerical approaches for solving problems in Figures 1a and 2a become highly inefficient and lack physical insight. In

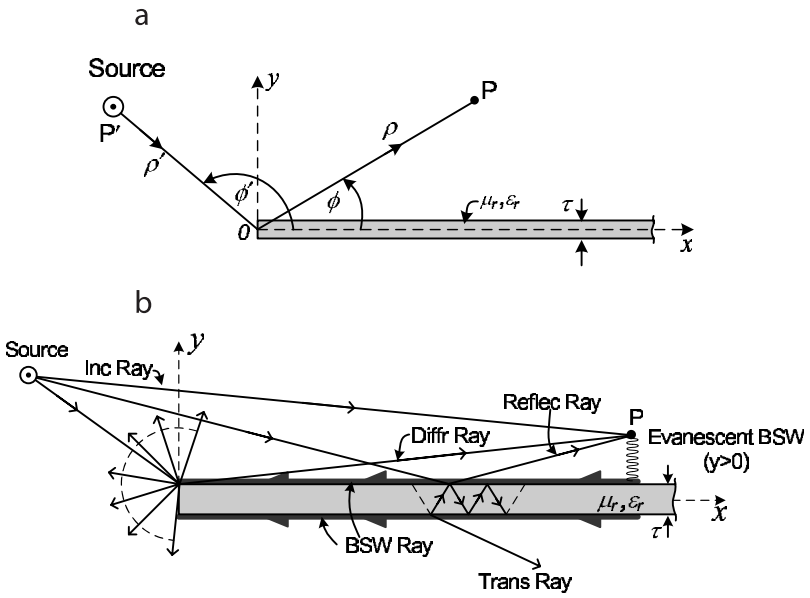

Figure 2. Thin, DPS/DNG material half plane illuminated by a line source. (a) A line source excitation. (b) Ray mechanisms.

1944799x, 2007, 6, Downloaded from https://agupubs.onlinelibrary.wiley.com/doi/10.1029/2007RS003689, Wiley Online Library on [23/02/2023]. See the Terms and Conditions (https://onlinelibrary.wiley.com/terms-and-conditions) on Wiley Online Library for rules of use; OA articles are governed by the applicable Creative Commons License

contrast, the present work, based on a heuristic spectral synthesis method, provides relatively simple closed form solutions that describe, in a physically appealing manner, the fields associated with the various UTD ray contributions, namely, the geometrical optics (GO), surface wave, and diffraction effects, respectively, which contribute to an observation point as shown in Figures 1b and 2b. It is noted that while the source may be near, or on, or far from the surface, it must remain at a distance which is somewhat larger than a free space wavelength from the discontinuity at "0". When the source is sufficiently far from the discontinuity and from the material surface, and when this source is a line dipole in which the direction of the dipole axis is oriented (or pointed) either directly toward the discontinuity, or close to that direction, then the UTD slope diffraction phenomena dominates over the first-order UTD based diffraction effects. In this case, the pattern of the field incident on the discontinuity from the line dipole is rapidly varying in angle as measured from the dipole axis on which its radiation pattern exhibits a null. One notes that the first-order UTD diffracted field is proportional to the value of the incident field at the discontinuity, while the slope diffraction is proportional to the derivative (slope) of the angular variation of the incident field at the discontinuity; hence, the slope effect alone remains dominant when the first-order diffraction either vanishes or becomes small in comparison. Furthermore, it is important to note that the first-order UTD ray field directly incident from a line source, or a line dipole source, which is placed either in or directly on a DPS/DNG material also vanishes along the material interface in accordance with the Karp-Karal lemma [*Zucker*, 1969], irrespective of the dipole orientation, but again the slope of the field incident from the source in this case does not. Thus, in the latter case, which arises for antennas placed on a DPS/DNG material, the space wave excited directly by the source also undergoes slope diffraction at the discontinuity, in addition to surface wave diffraction which also exists if that source is able to directly excite a surface wave (SW) in the material. Clearly, slope diffraction effects are therefore very important in most practical antenna and scattering problems involving material discontinuities. It is noted that DPS materials typically excite forward surface waves (FSWs), while DNG materials can support backward surface waves (BSWs) [*Engheta and Ziolkowski*, 2005]. BSWs are also included in the UTD solution developed below.

[3] Most previous works in the literature dealing with the diffraction by material discontinuities generally replace the original coated metallic surfaces or material slabs by approximate impedance or transmissive (for the geometry of Figure 2) boundary conditions, respectively, in order to arrive at a rigorous analytical solution to the resulting approximate problem configuration. These previous works primarily addresses the scattering problem in which the illumination is a uniform plane wave that is incident on the thin material discontinuity. In contrast, the present work applies not only to scattering situations but also to antenna problems which are of equally great practical importance. Moreover, slope diffraction effects were not treated in almost all previous works on the problems of scattering by material discontinuities, since the illumination used therein was typically a uniform plane wave. The present work incorporates plane, cylindrical, and surface wave illumination. Among related previous works, the one by *Tiberio et al.* [1989] provides a cylindrical or plane wave diffraction by a 2-D impedance wedge; and another paper by *Manara et al.* [1993] analyzes surface wave diffraction by the same geometry. However, although valid for the more general wedge geometry, those solutions in *Tiberio et al.* [1989] and *Manara et al.* [1993] are given in terms of rather complicated Maliuzhinets functions. Some initial, useful, related work is discussed by *Burnside and Burgener* [1983] where the earlier work by *Kouyoumjian and Pathak* [1974] for a perfectly conducting wedge is generalized heuristically for constructing a UTD solution for the diffraction by a DPS material half plane; however, the resulting diffracted field is non reciprocal and does not satisfy the Karp-Karal lemma on the material half plane; also, the solution does not contain surface wave (SW) effects. In *Luebbers* [1989] and *Nechayev and Constantinou* [2006], the work of *Burnside and Burgener* [1983] is directly extended to study the approximate UTD scattering by a wedge with impedance boundary conditions; these solutions also suffer from the same limitations as those in *Burnside and Burgener* [1983]. A W-H solution is available in *Volakis* [1988] for the plane wave diffraction by a thin DPS material half plane modeled using an approximate transmissive boundary condition. Also *Rojas and Pathak* [1989] analyzed the plane wave diffraction by a junction formed by a thin, planar two-part DPS material backed by an infinite ground plane which was modeled approximately by higher-order impedance boundary conditions on either side of the junction, respectively. Unlike the W-H and Maliuzhinets type solutions based on the impedance type approximation, the present solutions recover the proper, local plane wave Fresnel reflection and transmission coefficients (FRTCs), and surface wave constants, respectively, for the actual material. More importantly, the expressions for the first-order UTD as well as slope diffracted UTD fields obtained in this paper remain free of the complicated integral forms of the W-H split (or factorization) functions, and they also remain free of any complicated Maliuzhinets functions.

[4] In this paper, the solutions to the problems in Figures 1 and 2 are formulated initially in terms of a cylindrical wave spectral (CWS) integral for the scattered

1944799x, 2007, 6, Downloaded from https://agupubs.onlinelibrary.wiley.com/doi/10.1029/2007RS003689, Wiley Online Library on [23/02/2023]. See the Terms and Conditions (https://onlinelibrary.wiley.com/terms-and-conditions) on Wiley Online Library for rules of use; OA articles are governed by the applicable Creative Commons License

field (satisfying the wave equation). First the spectral weight function in the CWS for the problem in Figure 1 is synthesized heuristically based on an ansatz provided by the W-H solution to a special canonical problem of the plane wave diffraction by a two part impedance surface [*Rojas and Pathak*, 1989]. A bisection method, also described by *Rojas and Pathak* [1989], can be employed to directly synthesize a CWS for the problem in Figure 2 in terms of the CWS for the problem in Figure 1.

[5] This paper is organized as follows. Section 2 summarizes UTD ray solutions for the problem in Figure 1, including the slope diffraction terms. The UTD for the launching and diffraction of SWs is also discussed later in that section. The radiation and scattering from canonical problems of interest is calculated in section 3 using the UTD solutions obtained here, and are shown to compare very well with the modified W-H solutions obtained from *Volakis* [1988] and *Rojas and Pathak* [1989], which were developed originally to deal with very thin DPS materials via approximate boundary conditions. The case of a surface wave type antenna on a thin finite material strip, with a perfect electric conductor (PEC) backing is also analyzed via the UTD based on the results presented in section 2. It is noted that all the fields in this work are assumed to have an $e^{j\omega t}$ time dependence which is suppressed throughout the paper.

[6] Although this paper analyzes 2-D configurations, the corresponding 2-D UTD solutions developed here serve as crucial building blocks for constructing the related three-dimensional (3-D) configurations involving point source (or spherical wave) excitation of the geometries in Figures 1 and 2, respectively. The latter 3-D analysis is currently being completed; furthermore, it appears that the development of such 3-D solutions will not only solve more realistic problems, but would also potentially provide a physical picture, based on the UTD ray physics, for describing focusing effects in DNG flat lens geometries. The 3-D solutions pertaining to configurations in Figures 1 and 2, respectively, will be reported separately.

2. Development of the UTD Solution for Wave Diffraction by a Junction Between Two Different Planar DPS/DNG Material Slabs on a PEC Ground Plane

[7] The geometrical configuration of the problem of interest is shown in Figure 1a. A UTD solution to the problem in Figure 1a is obtained first in section 2.1 for the case of plane wave incidence. This solution is based on a useful ansatz which is provided by a heuristic simplification of the W-H solution to a related special canonical two-part impedance diffraction problem. The simplification in question involves the replacement of a term involving the W-H split functions with a constant term (unity). This replacement occurs within the steepest descent path (SDP) integral in W-H solution, and it greatly simplifies the solution. Next, in section 2.2, the ansatz of section 2.1 is extended to treat the case of line-source illumination. UTD slope-diffraction terms are introduced in section 2.3.

2.1. Ansatz for the Plane Wave Illumination Case

[8] For the sake of simplicity, and with no loss of generality, consider a special case of the geometry of Figure 1a in which the *o*-face is defined to be a uniform surface impedance (or admittance) whose value is Z_s^o (or Y_s^o) for the TM (or TE) case, respectively, while the *n*-face is just a PEC. Here, the *o*-face exists for $x > 0$ and $y = 0$, and the *n*-face exists for $x < 0$ and $y = 0$. When this special two-part geometry is illuminated by an incident, unit amplitude, plane wave field, u_{pw}^i, where u_{pw}^i is the incident electric (or magnetic) field $\hat{z}E_z^i$ (or $\hat{z}H_z^i$) for the TE (or TM) case, then the total field, u_{pw}^t for $y > 0$ (free space) may be expressed as

$$u_{pw}^t = u_{pw}^i + u_{pw}^s \tag{1}$$

where u_{pw}^t represents the total electric field $\hat{z}E_z$ for the TE case (or the total magnetic field $\hat{z}H_z$ for the TM case). The u_{pw}^s is the scattered field component corresponding to $\hat{z}E_z^s$ (or $\hat{z}H_z^s$) for the TE (or TM) case. It is noted that

$$u_{pw}^i = e^{jk\rho\cos(\phi-\phi')}. \tag{2}$$

[9] From the W-H solution for the canonical two part problem in *Rojas and Pathak* [1989], the u_{pw}^s at $P(\rho, \phi)$ is

$$u_{pw}^s = R_{e,h}^o(\phi')e^{jk\rho\cos(\phi+\phi')} + u_{pw}^p(\rho, \phi) \tag{3}$$

where k is free space wave number, and $R_{e,\,h}^o$ is the *o*-face reflection coefficient, namely

$$R_{e,h}^o(\phi') = \frac{\sin\phi' - \delta_{e,h}^o}{\sin\phi' + \delta_{e,h}^o}. \tag{4}$$

[10] It is noted that the special case of plane wave illumination of the discontinuity results when the line source at (ρ', ϕ') as in Figure 1a is allowed to recede to infinity (i.e. $\rho' \to \infty$). The first term on the right hand side (RHS) of (3) is chosen here to correspond to the field reflected from an "unperturbed" surface which is assumed to be an entire (infinite) plane at $y = 0$ characterized by the impedance Z_s^o (or admittance Y_s^o) for the TM (or TE) case. The $\delta_{e,\,h}^o$ in (4) are defined by $\delta_e^o = Y_s^o/Y_o$ and $\delta_h^o = Z_s^o/Z_o$, respectively, where Z_o ($= Y_o^{-1}$) is

1944799x, 2007, 6, Downloaded from https://agupubs.onlinelibrary.wiley.com/doi/10.1029/2007RS003689, Wiley Online Library on [23/02/2023]. See the Terms and Conditions (https://onlinelibrary.wiley.com/terms-and-conditions) on Wiley Online Library for rules of use; OA articles are governed by the applicable Creative Commons License

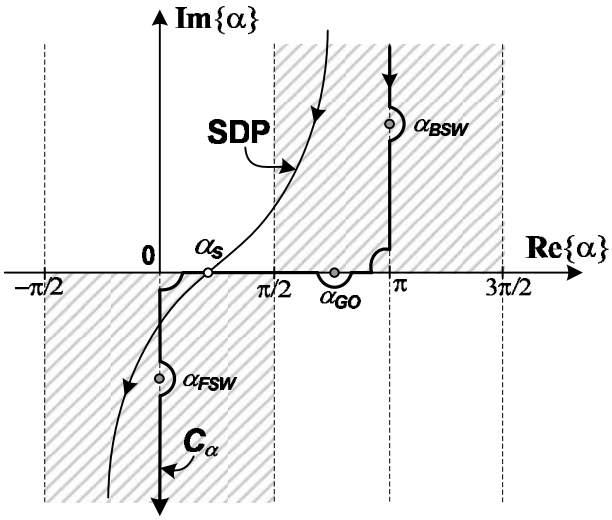

Figure 3. Deformation of the Sommerfeld contour C_α used in the spectral synthesis into the steepest descent path (SDP) in the α plane.

the free space impedance. Thus, the second term, u^p_{pw}, on the RHS of (3) constitutes a "perturbation" to the first term; it arises from the fact that the special geometry being considered is actually a two-part problem (of which one part, namely that for $x < 0$ and $y = 0$ is PEC) rather than just an "unperturbed" entire impedance (admittance) surface at $y = 0$. From *Rojas and Pathak* [1989], one obtains

$$u^p_{pw} = -\frac{1}{2\pi j}\int_{C_\alpha}\left[R^o_{e,h}(\phi') - R^n_{e,h}(\phi')\right] \cdot \Lambda_{e,h}(\alpha,\phi')e^{-jk\rho\cos(\alpha-\phi)}\,d\alpha \tag{5}$$

where

$$\Lambda_e = \left\{\frac{\sin\frac{\alpha}{2}}{\cos\frac{\phi'}{2}}\frac{G^e_-(k\cos\alpha)}{G^e_-(-k\cos\phi')}\right\} \cdot \left(+\frac{1}{2}\right)\left[\sec\left(\frac{\alpha-\phi'}{2}\right) + \sec\left(\frac{\alpha+\phi'}{2}\right)\right] \tag{6}$$

and

$$\Lambda_h = \left\{\frac{\cos\frac{\phi'}{2}}{\sin\frac{\alpha}{2}}\frac{G^h_-(k\cos\alpha)}{G^h_-(-k\cos\phi')}\right\} \cdot \left(-\frac{1}{2}\right)\left[\sec\left(\frac{\alpha-\phi'}{2}\right) - \sec\left(\frac{\alpha+\phi'}{2}\right)\right]. \tag{7}$$

[11] The contour C_α in the complex angular spectral α plane is shown in Figure 3; it is chosen to satisfy the radiation condition. In the above, the reflection coefficient $R^n_e(\phi') = -1$ and $R^n_h(\phi') = 1$ for the n-face because it is PEC in this canonical problem. The $G^{e,h}_+$ and $G^{e,h}_-$ constitute the W-H factors (or split functions) of the functions,

$$G^e(\alpha) = \frac{1}{k(\sin\alpha + Y_s/Y_o)}$$

and

$$G^h(\alpha) = \frac{\sin\alpha}{\sin\alpha + Z_s/Z_o},$$

respectively. The W-H factorization of $G^{e,h}(\alpha)$ into $G^{e,h}_+(\alpha)G^{e,h}_-(\alpha)$ leads to explicit expressions for the split functions in terms of an integral for each [*Rojas and Pathak*, 1989]. The spectral integral in (5) may be evaluated for large $k\rho$ via the method of steepest descent. Thus, deforming C_α into the steepest descent path (SDP) through the saddle point at $\alpha \equiv \alpha_s$ (= ϕ), as in Figure 3, allows one to obtain

$$u^p_{pw} = -\left[R^o_{e,h}(\phi') - R^n_{e,h}(\phi')\right] \cdot e^{jk\rho\cos(\phi+\phi')}U(\phi-\pi+\phi') - u^{sw}_{pw}U_{sw} - \frac{1}{2\pi j}\int_{SDP}\left[R^o_{e,h}(\phi') - R^n_{e,h}(\phi')\right]\Lambda_{e,h}(\alpha,\phi') \cdot e^{-jk\rho\cos(\alpha-\phi)}\,d\alpha. \tag{8}$$

[12] The first term involving $[R^o_{e,h} - R^n_{e,h}]e^{jk\rho\cos(\phi+\phi')}$ on the RHS of (8) is $2\pi j$ times the residue arising from crossing the GO pole of $\sec(\frac{\alpha+\phi'}{2})$ at $\alpha \equiv \alpha_{go} = \pi - \phi'$ in deforming C_α to SDP. Likewise, the second term u^{sw}_{pw} is the surface wave (SW) field launched on the o-face via diffraction by the discontinuity at "0"; it is given by $2\pi j$ times the residue arising from a capture of the SW pole of $G^{e,h}_-(k\cos\alpha)$ at $\alpha = \alpha_{sw}$ in this contour deformation. The $U(\cdot)$ is the Heaviside step function whose value is unity for positive arguments and zero for negative arguments. Also U_{sw} is a step function which is unity if a surface wave pole is captured; otherwise it is zero.

[13] A heuristic approximation, based on a set of physical arguments enumerated below, can be introduced in (8) to remove the cumbersome W-H split functions $G^{e,h}_-$. In the vicinity of the RSB, where the saddle point $\alpha_s = \phi$ approaches $\pi - \phi'$, the dominant contribution to the SDP integral in (8) comes from a region where $\sec(\frac{\alpha_s+\phi'}{2})$ approaches a singularity, and within this region the bracketed term that involves the ratio of the W-H split

1944799x, 2007, 6, Downloaded from https://agupubs.onlinelibrary.wiley.com/doi/10.1029/2007RS003689, Wiley Online Library on [23/02/2023]. See the Terms and Conditions (https://onlinelibrary.wiley.com/terms-and-conditions) on Wiley Online Library for rules of use; OA articles are governed by the applicable Creative Commons License

functions $\frac{G_-^{e,h}(k\cos\alpha_s)}{G_-^{e,h}(-k\cos\phi')}$ can be approximated by unity. Thus, one obtains a simplified form for u_{pw}^p as follows:

$$u_{pw}^p \cong -\frac{1}{2\pi j}\int_{C_\alpha} d\alpha\left[R_{e,h}^o(\alpha)-R_{e,h}^n(\alpha)\right]\left(\pm\frac{1}{2}\right)\cdot\left[\sec\left(\frac{\alpha-\phi'}{2}\right)\pm\sec\left(\frac{\alpha+\phi'}{2}\right)\right]e^{-jk\rho\cos(\alpha-\phi)}. \tag{9}$$

[14] It is important to note that the $R_{e,h}^o(\phi')$ and $R_{e,h}^n(\phi')$ in (5) are now replaced by $R_{e,h}^o(\alpha)$ and $R_{e,h}^n(\alpha)$, respectively, in (9). The latter is necessary because α_{sw} is a pole of $G_-^{e,h}(\alpha)$ in the integrand of (5), and to preserve this important property in the approximate integrand of (9) (which is now devoid of $G_-^{e,h}(\alpha)$) it is necessary to have it manifest as a pole at $\alpha = \alpha_{sw}$ of the spectral reflection coefficient $R_{e,h}^o(\alpha)$ in (9) for the *o*-face. Of course, $R_{e,h}^n(\alpha) = \mp 1$, as before for the PEC *n*-face. Deforming C_α into the SDP contour allows one to express (9) as

$$u_{pw}^p \cong -\left[R_{e,h}^o(\phi')-R_{e,h}^n(\phi')\right]\cdot e^{jk\rho\cos(\phi+\phi')}U(\phi-\pi+\phi')-\tilde{u}_{pw}^{sw}U_{sw} -\frac{1}{2\pi j}\int_{SDP} d\alpha\left[R_{e,h}^o(\alpha)-R_{e,h}^n(\alpha)\right]\left(\pm\frac{1}{2}\right)\cdot\left[\sec\left(\frac{\alpha-\phi'}{2}\right)\pm\sec\left(\frac{\alpha+\phi'}{2}\right)\right]e^{-jk\rho\cos(\alpha-\phi)}. \tag{10}$$

[15] One notes that the $\tilde{u}_{pw}^{sw}$ in (10) is now an approximation to u_{pw}^{sw} of (8); likewise, the SDP integral in (10) is an approximation to the SDP integral of (8). Nevertheless, the approximation result in (10) contains the same GO pole contribution and the surface wave propagation constant as does the exact W-H result in (8). Also, a closed from evaluation of the SDP integral in (10) via the non-uniform steepest descent method, yields the diffracted field $\tilde{u}_{pw}^d$ given by

$$\tilde{u}_{pw}^d \sim -\frac{e^{-j\pi/4}}{\sqrt{2\pi k}}\left[R_{e,h}^o(\phi)-R_{e,h}^n(\phi)\right]\left(\pm\frac{1}{2}\right)\cdot\left[\sec\left(\frac{\phi-\phi'}{2}\right)\pm\sec\left(\frac{\phi+\phi'}{2}\right)\right]\frac{e^{-jk\rho}}{\sqrt{\rho}}, \tag{11}$$

which still continues to satisfy the PEC boundary condition on the *n*-face and the Karp-Karal lemma on the *o*-face, respectively despite the approximations used to arrive at (9). Thus, the solution in (10) (and (11)), which is based on the approximate expression of (9), clearly retains many of the important physical properties which are present in the corresponding exact W-H result of (8), thereby lending more confidence to the heuristic approximation of (9). In contrast, a solution based on a Kirchhoff type approximation generally will not retain most of the above properties.

[16] While u_{pw}^d, based on the W-H method, satisfies reciprocity, the approximate diffracted $\tilde{u}_{pw}^d$ of (11) does not; it will be shown later in section 2.2 how reciprocity can be restored into $\tilde{u}_{pw}^d$ in very simple fashion. As expected, the non-uniform results for u_{pw}^d and $\tilde{u}_{pw}^d$, respectively, become unbounded at the RSB. Bounded results for these diffracted fields can be easily obtained in terms of the UTD Fresnel integral type transition functions via a uniform asymptotic evaluation of the SDP integrals. The latter uniform approach has not been incorporated above as it is not essential for arriving at the desired ansatz; it will be employed later in section 2.2 when developing the UTD solution for the original problem in Figure 1a. The desired ansatz is now established by the set of equations (1)–(4) and (9), respectively.

2.2. Extension to Treat the Uniform Line Source Excitation Case

[17] The problem treated below is that of a uniform line source excitation of a junction between two semi-infinite, thin, planar DPS/DNG material slabs of different electrical properties and thickness on a PEC ground plane as shown in Figure 1. The incident, $\hat{z}$-directed, electric field, E_z^i, (or the magnetic field, H_z^i) at an observer location $\bar{\rho}(\rho,\ \phi)$, which is produced by a uniform electric (or magnetic) line source of strength I_o (or M_o) at $\bar{\rho}'(\rho',\ \phi')$, respectively, can be expressed as [*Felsen and Marcuvitz*, 1994]

$$u^i \equiv \begin{Bmatrix} E_z^i \\ H_z^i \end{Bmatrix} = -jk\begin{Bmatrix} Z_oI_o \\ Y_oM_o \end{Bmatrix}G_o(k|\bar{\rho}-\bar{\rho}'|) \tag{12}$$

$$G_o(k|\bar{\rho}-\bar{\rho}'|) = \frac{-j}{4}H_o^{(2)}(k|\bar{\rho}-\bar{\rho}'|) \tag{13}$$

where $H_o^{(2)}$ is a Hankel function of the second kind and order zero. The $\bar{\rho}$ and $\bar{\rho}'$ are shown in Figure 1a. For sufficiently large $k\rho'$ (i.e. for source not close to the discontinuity at "0" which is assumed true), G_o may be replaced by its large argument form, namely

$$G_o(kS^i) \sim \frac{-j}{4}\sqrt{\frac{2j}{\pi k}}\frac{e^{-jkS^i}}{\sqrt{S^i}}. \tag{14}$$

where $|\bar{\rho}-\bar{\rho}'| = S^i$, and

$$S^i = \sqrt{\rho^2+\rho'^2-2\rho\rho'\cos(\phi-\phi')}. \tag{15}$$

1944799x, 2007, 6, Downloaded from https://agupubs.onlinelibrary.wiley.com/doi/10.1029/2007RS003689, Wiley Online Library on [23/02/2023]. See the Terms and Conditions (https://onlinelibrary.wiley.com/terms-and-conditions) on Wiley Online Library for rules of use; OA articles are governed by the applicable Creative Commons License

[18] The solution for the total field u^t, which corresponds to $\hat{z}E_z$ (or $\hat{z}H_z$) for the TE (or TM) case, for the problem Figure 1a, may be based on the ansatz established in (1)–(4) and (9) as described above. Following (1), one may express

$$u^t = u^i + u^s \tag{16}$$

where the scattered field u^s for the geometry in Figure 1a can be decomposed as in (3), if one assumes that the line source is sufficiently far from the o and n faces, respectively. Thus, under the latter assumption,

$$u^s \cong -\frac{k}{4}\left\{ \begin{array}{c} Z_o I_o \\ Y_o M_o \end{array} \right\} \sqrt{\frac{2j}{\pi k}} \mathcal{R}^o_{e,h}(\phi') \frac{e^{-jkS^r}}{\sqrt{S^r}} + u^p(\rho, \phi) \tag{17}$$

where, as in (3), the first term on the RHS of (17) represents the field scattered from the "unperturbed" structure, which is assumed to be an infinite planar structure consists of a thin PEC backed material that is identical (in its geometrical and electrical properties) to the original PEC backed material pertaining to the o-face in Figure 1a. Under the present assumption of source far from the surface at $y = 0$, one can show that the unperturbed scattered field is asymptotically given by the first term on the RHS of (17) which is the GO reflected field, where $\mathcal{R}^o_{e,h}$ is the Fresnel reflection coefficient (FRC) for this unperturbed surface, and S^r is the GO ray path corresponding to the GO field reflected from that unperturbed surface, where

$$\mathcal{R}^o_{e,h}(\phi') = \frac{P^o_{e,h}(\phi')}{Q^o_{e,h}(\phi')} \tag{18}$$

with

$$P^o_{e,h}(\phi') = \left\{ \left[\sin\phi' - \eta_{e,h}\mathcal{N}(\phi')\right] \mp \left[\sin\phi' + \eta_{e,h}\mathcal{N}(\phi')\right] \cdot e^{-j2k\tau_o \mathcal{N}(\phi')} \right\} e^{j2k\tau_o \sin\phi'} \tag{19}$$

and

$$Q^o_{e,h}(\phi') = \left[\sin\phi' + \eta_{e,h}\mathcal{N}(\phi')\right] \mp \left[\sin\phi' - \eta_{e,h}\mathcal{N}(\phi')\right] \cdot e^{-j2k\tau_o \mathcal{N}(\phi')}. \tag{20}$$

Also,

$$\mathcal{N}(\phi') = \sqrt{\mu_r \epsilon_r - \cos^2\phi'}. \tag{21}$$

[19] In the above, τ_o is the material thickness for the o-face, and $\eta_e = 1/\mu_r$ for the TE (or e) case, while $\eta_h = 1/\epsilon_r$ for the TM (or h) case, respectively. Also,

$$S^r = \sqrt{\rho^2 + \rho'^2 - 2\rho\rho'\cos(\phi + \phi')}. \tag{22}$$

[20] As in (3), the $u^p(\rho, \phi)$ represents the "perturbation" to the first term on the RHS of (17); it arises from the fact that the actual geometry in Figure 1a is composed of two different PEC backed materials on the o and n faces, instead of a single "unperturbed" surface. The $u^p(\rho, \phi)$ can be expressed as a CWS integral [*Pathak and Kouyoumjian*, 1970] by

$$u^p = -\frac{1}{2\pi j}\int_{C_\alpha} \mathcal{A}_{e,h}(\alpha, \phi') G_o[kS(\alpha)]\, d\alpha. \tag{23}$$

[21] In (23), the $\mathcal{A}_{e,\ h}(\alpha)$ is the appropriate spectral amplitude or weight function, and $G_o[kS(\alpha)]$ denotes the CWS kernel based on the free space line source Green's function, namely, $G_o[kS(\alpha)] = \frac{-j}{4}H^{(2)}_o[kS(\alpha)]$ with

$$S(\alpha) = \sqrt{\rho^2 + \rho'^2 + 2\rho\rho'\cos(\alpha - \phi)}. \tag{24}$$

[22] It is important to note that if the line source is not assumed to be sufficiently far from the o and n faces, then additional contributions (not present in (17)) must be included. Such additional contributions arise because the line source can excite SWs directly in the material; these SWs become incident on the discontinuity at "0" to produce a reflected SW and a transmitted SW, as well as a diffracted space wave. The reflected and transmitted SWs can be deduced from the W-H solution to appropriate, simpler, canonical two-part diffraction problems in which the excitation is an incident SW. In the radiation problem, these SW effects are not significant. The latter will be reported in a separate paper. Only the diffraction of the incident SW by the discontinuity contributes to the radiation field; its effect is discussed separately in section 2.3. The $G_o[kS(\alpha)]$ in (23) may now be replaced by its large argument form valid for large $k\rho'$ (or $k\rho$) as

$$G_o[kS(\alpha)] \sim \frac{-j}{4}\sqrt{\frac{2j}{\pi k}}\frac{e^{-jkS(\alpha)}}{\sqrt{S(\alpha)}}. \tag{25}$$

[23] The spectral function $\mathcal{A}_{e,h}$ is proportional to the strength of the line source, and may be expressed as

$$\mathcal{A}_{e,h}(\alpha, \phi') \equiv -jk\left\{ \begin{array}{c} Z_o I_o \\ Y_o M_o \end{array} \right\} \mathcal{D}^c_{e,h}(\alpha, \phi') \tag{26}$$

where the unknown spectral weight $\mathcal{D}^c_{e,h}$ is to be determined using the ansatz of section 2.1 based on the special canonical problem which retains all the features of the original problem in Figure 1a. In order to identify $\mathcal{D}^c_{e,h}$, the exponential in (25) may be approximated by the first two terms of its binomial expansion for large $k\frac{\rho\rho'}{\rho+\rho'}$, which is assumed here to be the large parameter

1944799x, 2007, 6, Downloaded from https://agupubs.onlinelibrary.wiley.com/doi/10.1029/2007RS003689, Wiley Online Library on [23/02/2023]. See the Terms and Conditions (https://onlinelibrary.wiley.com/terms-and-conditions) on Wiley Online Library for rules of use; OA articles are governed by the applicable Creative Commons License

(for the asymptotic development). Then, (23) becomes

$$u^p(\rho,\phi) = -\frac{1}{2\pi j}\int_{C_\alpha} \mathcal{A}_{e,h}(\alpha,\phi')\left(\frac{-j}{4}\sqrt{\frac{2j}{\pi k}}\right) \cdot \frac{e^{-jk(\rho+\rho')}}{\sqrt{S(\alpha)}} e^{jk\frac{\rho\rho'}{\rho+\rho'}[1-\cos(\alpha-\phi)]}\, d\alpha. \quad (27)$$

[24] If the line source is allowed to receded to infinity, i.e., if $\rho' \to \infty$, while ρ is kept finite, then one obtains the scattered field u^p_{pw} due to plane wave illumination, namely

$$u^p(\rho,\phi) \sim C_o(k\rho')u^p_{pw} \quad (28)$$

where C_o is the line source factor given by

$$C_o(k\rho') = -jk\left\{\begin{array}{c} Z_oI_o \\ Y_oM_o \end{array}\right\}\frac{-j}{4}\sqrt{\frac{2j}{\pi k}}\frac{e^{-jk\rho'}}{\sqrt{\rho'}} \quad (29)$$

and

$$u^p_{pw} = -\frac{1}{2\pi j}\int_{C_\alpha} \mathcal{D}^c_{e,h}(\alpha,\phi')e^{-jk\rho\cos(\alpha-\phi)}\, d\alpha. \quad (30)$$

[25] By directly comparing (30) with the desired ansatz in (9), one can easily identify $\mathcal{D}^c_{e,h}$ by inspection to be

$$\mathcal{D}^c_{e,h}(\alpha,\phi') = \pm\frac{1}{2}\left[\mathcal{R}^o_{e,h}(\alpha) - \mathcal{R}^n_{e,h}(\alpha)\right] \cdot \left[\sec\left(\frac{\alpha-\phi'}{2}\right) \pm \sec\left(\frac{\alpha+\phi'}{2}\right)\right], \quad (31)$$

except that new material FRCs $\mathcal{R}^{o,n}_{e,h}$ must now be used in (31) to replace $R^{o,n}_{e,h}$ of (9) pertaining to the two part impedance boundary approximation of the W-H solution. The $\mathcal{R}^o_{e,h}(\alpha)$ is defined in (18) with ϕ' replaced by α in (31), and $\mathcal{R}^n_{e,h}(\alpha)$ is likewise the spectral FRC for the n-face at ($x < 0$, $y = 0$). Here $\mathcal{R}^{o,n}_{e,h}(\alpha) = \frac{P^{o,n}_{e,h}(\alpha)}{Q^{o,n}_{e,h}(\alpha)}$, where $P^{o,n}_{e,h}(\alpha) = \{[\sin\alpha - \eta_{e,h}\mathcal{N}(\alpha)] \mp [\sin\alpha + \eta_{e,h}\mathcal{N}(\alpha)]e^{-j2k\tau\mathcal{N}(\alpha)}\}e^{j2k\tau\sin\alpha}$, and $Q^{o,n}_{e,h}(\alpha) = [\sin\alpha + \eta_{e,h}\mathcal{N}(\alpha)] \mp [\sin\alpha - \eta_{e,h}\mathcal{N}(\alpha)]e^{-j2k\tau\mathcal{N}(\alpha)}$ with the slab thickness $\tau = \tau_o$ for the o-face and $\tau = \tau_n$ for the n-face. It is noted that if one removes the material slab for $x > 0$ (or $x < 0$), then the $\mathcal{R}^o_{e,h}$ (or $\mathcal{R}^n_{e,h}$) automatically reduces to (∓ 1) for the PEC case pertaining to the $\binom{e}{h}$ polarization. The $\eta_e = 1/\mu_r$ for TE (e) case, $\eta_h = 1/\epsilon_r$ for TM (h) case, and $\mathcal{N}(\alpha) = \sqrt{\epsilon_r\mu_r - \cos^2\alpha}$ as before. The $\mathcal{R}^{o,n}_{e,h}(\alpha)$ term yields the proper material FRC for describing the GO reflected field from the residue of the GO pole at $\alpha = \alpha_{go} = \pi - \phi'$ in (27) (together with (31)) where the $\sec(\frac{\alpha+\phi'}{2})$ function in $\mathcal{D}^c_{e,h}(\alpha, \phi')$ becomes singular.

[26] After deforming the integral contour of (27) to the steepest descent path (SDP) through the saddle point at $\alpha \equiv \alpha_s = \phi$ as shown in Figure 3, one defines the SDP integral, which yields the diffracted field u^d, to be

$$u^d = \int_{SDP} \mathcal{F}_{e,h}(\alpha,\phi')e^{\kappa f(\alpha)}\, d\alpha, \quad (32)$$

where

$$\mathcal{F}_{e,h}(\alpha,\phi') = \frac{k}{8\pi j}\left\{\begin{array}{c} Z_oI_o \\ Y_oM_o \end{array}\right\}\sqrt{\frac{2j}{\pi k}} \cdot \mathcal{D}^c_{e,h}(\alpha,\phi')\frac{e^{-jk(\rho+\rho')}}{\sqrt{S(\alpha)}},$$

the κ denotes $k\frac{\rho\rho'}{\rho+\rho'}$, and $f(\alpha) = j[1 - \cos(\alpha - \phi)]$. It is noted that in (27) (together with (31)), the $\alpha = \alpha_{sw}$ marks the location of the SW pole where the denominator of $\mathcal{R}^{o,n}_{e,h}$ in $\mathcal{D}^c_{e,h}(\alpha, \phi')$ vanishes. This leads to an exact form of the transcendental or characteristic equation for the SWs which may be of the FSW or BSW type, respectively. Since the saddle point at $\alpha \equiv \alpha_s = \phi$ moves with the observation point, the pole at α_{go} is captured to provide a non zero GO reflected field u^r where $u^r = u^{ro}$ for the o-face when $\phi + \phi' < \pi$ and $u^r = u^{rn}$ for the n-face when $\phi + \phi' > \pi$. The residue from the pole at α_{sw} yields either a FSW or a BSW field contribution, u^{sw}. The integral along the SDP in (32) may be evaluated asymptotically in a uniform fashion for large κ to yield the UTD closed form expression for the diffracted field contribution u^d. It is desirable to decompose the spectral function in the integrand of (32) into a term containing only GO pole singularities and a term containing only SW pole singularities. Such a decomposition allows one to conveniently obtain the GO dominant UTD diffraction coefficient from the spectral part containing the GO type pole in a simple form using the Pauli-Clemmow (PC) approach [*Pathak and Kouyoumjian*, 1970], while the remainder spectral part can be treated by the Van der Waerden (VDW) approach [*Felsen and Marcuvitz*, 1994]. The total field u^t for corresponding DPS/DNG material configuration at an observation point (P) or at (ρ, ϕ) may be expressed via (16), (17) and (32) as the sum of the classical line source incident field (with target absent) and scattered field, i.e., $u^t(\rho, \phi) = u^i + u^s$, in which $u^s = u^r + u^{sw} + u^d$. The u^d denotes the first-order diffracted field emanating from the material discontinuity at "0", and u^{sw} denotes the FSW/BSW field along the o or n-face after being launched at "0". Note that the classical incident field is given asymptotically (for $k\rho' \gg 1$) by (12) (together with (14)). Since $0 < \phi, \phi' < \pi$, the u^i is also the GO incident field for $y > 0$. The reflected field u^r is given

1944799x, 2007, 6, Downloaded from https://agupubs.onlinelibrary.wiley.com/doi/10.1029/2007RS003689, Wiley Online Library on [23/02/2023]. See the Terms and Conditions (https://onlinelibrary.wiley.com/terms-and-conditions) on Wiley Online Library for rules of use; OA articles are governed by the applicable Creative Commons License

by the sum of the "unperturbed" GO reflected field contained in the first term on the RHS of (17) and the pole contribution from $\alpha = \alpha_{go} = \pi - \phi'$ in (27) (together with (26) and (31)) given by $\frac{k}{4}\begin{pmatrix} Z_o I_o \\ Y_o M_o \end{pmatrix}\sqrt{\frac{2j}{\pi k}}\,[\mathcal{R}^o_{e,h}(\phi') - \mathcal{R}^n_{e,\,h}(\phi')]\; U[\phi - (\pi - \phi')]$ as

$$u^r(\rho,\phi) = -\frac{k}{4}\begin{Bmatrix} Z_o I_o \\ Y_o M_o \end{Bmatrix}\sqrt{\frac{2j}{\pi k}}\mathcal{R}_{e,h}(\phi')\frac{e^{-jkS_r}}{\sqrt{S_r}} \tag{33}$$

where $S_r = \sqrt{\rho^2 + \rho'^2 - 2\rho\rho'\cos(\phi + \phi')}$, and

$$\mathcal{R}_{e,h}(\phi') = \begin{cases} \mathcal{R}^o_{e,h}(\phi') = \dfrac{P^o_{e,h}(\phi')}{Q^o_{e,h}(\phi')}, & \phi + \phi' < \pi \\ \mathcal{R}^n_{e,h}(\phi') = \dfrac{P^n_{e,h}(\phi')}{Q^n_{e,h}(\phi')}, & \phi + \phi' > \pi \end{cases} \tag{34}$$

in which $\mathcal{R}^{o,n}_{e,h}$ denotes the FRC. Also, u^{sw} is given by the pole contribution from $\alpha = \alpha_{sw}$ to (27) as

$$\begin{aligned} u^{sw}(\rho,\phi) = -\frac{k}{4}\begin{Bmatrix} Z_o I_o \\ Y_o M_o \end{Bmatrix}\sqrt{\frac{2j}{\pi k}} \\ \cdot \left[R^{swo}_{e,h}\left(\alpha^o_{sw},\phi'\right)\frac{e^{-jkS\left(\alpha^o_{sw},\phi\right)}}{\sqrt{S\left(\alpha^o_{sw},\phi\right)}}U\left(\phi^o_{sw} - \phi\right)\right. \\ - R^{swn}_{e,h}\left(\alpha^n_{sw},\phi'\right)\frac{e^{-jkS\left(\alpha^n_{sw},\phi\right)}}{\sqrt{S\left(\alpha^n_{sw},\phi\right)}} \\ \left. \cdot U\left(\phi^n_{sw} - [\pi - \phi]\right)\right] \end{aligned} \tag{35}$$

where $\phi^{o,n}_{sw}$ (and $\alpha^{o,n}_{sw}$) denote ϕ_{sw} (and α_{sw}) for the (o, n) face. Here,

$$\phi_{sw} = \begin{cases} \cos^{-1}\left(\dfrac{1}{\cosh\xi_{sw}}\right) & \text{, for } \alpha_{sw} = -j\xi_{sw} \\ \pi - \cos^{-1}\left(\dfrac{1}{\cosh\xi_{sw}}\right) & \text{, for } \alpha_{sw} = \pi + j\xi_{sw} \end{cases}. \tag{36}$$

[27] It is noted that $\alpha_{sw} = -j\xi_{sw}$ case is for FSW, and $\alpha_{sw} = \pi + j\xi_{sw}$ is for BSW, respectively. Also,

$$\begin{aligned} R^{swo}_{e,h}\left(\alpha^o_{sw},\phi'\right) = \pm\frac{P^o_{e,h}\left(\alpha^o_{sw}\right)}{2Q^{o'}_{e,h}\left(\alpha^o_{sw}\right)} \\ \cdot \left[\sec\left(\frac{\alpha^o_{sw} - \phi'}{2}\right) \pm \sec\left(\frac{\alpha^o_{sw} + \phi'}{2}\right)\right]. \end{aligned} \tag{37}$$

[28] The $Q^{o'}_{e,h}(\alpha_{sw})$ is the derivative of $Q^o_{e,h}(\alpha)$ with respect to α and evaluated at $\alpha = \alpha_{sw}$. The $U(\cdot)$ denotes the Heaviside unit step function as before. The $R^{swn}_{e,h}(\alpha^n_{sw}, \phi')$ is given by (37) with o replaced by n, likewise, $S(\alpha^o_{sw}, \phi) = \sqrt{\rho^2 + \rho'^2 + 2\rho\rho'\cos\left(\alpha^o_{sw} - \phi\right)}$ and $S(\alpha^n_{sw}, \phi)$ can be found similarly. The expressions for the UTD first-order diffracted field is given by

$$u^d(\rho,\phi) = u^i(0)D_{e,h}(\phi,\phi')\frac{e^{-jk\rho}}{\sqrt{\rho}} \tag{38}$$

where $D_{e,h} = D^{go}_{e,h} + D^{sw}_{e,h}$. Here $u^i(0)$ denotes the GO incident field at the diffraction point corresponding to the discontinuity at "0" (see Figure 1a). The $D^{go}_{e,h}$ is based on the PC method and $D^{sw}_{e,h}$ is based on the VDW method as explained previously; they are given by

$$\begin{aligned} D^{go}_{e,h}(\phi,\phi') = \mp\frac{e^{-j\pi/4}}{2\sqrt{2\pi k}}\left[\Gamma^o_{e,h}(\phi,\phi') - \Gamma^n_{e,h}(\phi,\phi')\right] \\ \cdot \left[\sec\left(\frac{\phi - \phi'}{2}\right)F_{KP}\left(kLa^-_{go}\right)\right. \\ \left. \pm \sec\left(\frac{\phi + \phi'}{2}\right)F_{KP}\left(kLa^+_{go}\right)\right], \end{aligned} \tag{39}$$

where $a^{\pm}_{go} = 2\cos^2(\frac{\phi \pm \phi'}{2})$ and $L = \frac{\rho'\rho}{\rho' + \rho}$. The function $F_{KP}(x)$ is the well-known UTD edge transition function defined by *Kouyoumjian and Pathak* [1974]. The proper branch of $\sqrt{kLa}$ is chosen such that $-\frac{3\pi}{4} < arg(\sqrt{kLa}) < \frac{\pi}{4}$, where $a = a^{\pm}_{go}$, to satisfy the radiation condition. The $\Gamma^{o,n}_{e,h}(\phi, \phi')$ is an ad hoc modification to $\mathcal{R}^{o,n}_{e,h}(\alpha)$ such that $\sin\alpha$ in the latter is split into $2\sin(\alpha/2)\sin(\phi'/2)$ so as to preserve reciprocity (symmetry) in $D^{go}_{e,h}$ with respect to ϕ and ϕ' when $\alpha = \phi$ at the saddle point, and to also let $\Gamma^{o,\,n}_{e,\,h}(\phi, \phi')$ reduces exactly to $\mathcal{R}^{o,n}_{e,h}(\alpha)$ at the GO reflection shadow boundary ($\alpha = \phi = \pi - \phi'$) as it should. Thus,

$$\Gamma^{o,n}_{e,h}(\phi,\phi') = \frac{\left[\zeta - \eta_{e,h}N\right] \mp \left[\zeta + \eta_{e,h}N\right]e^{-j2k\tau_{o,n}N}}{\left[\zeta + \eta_{e,h}N\right] \mp \left[\zeta - \eta_{e,h}N\right]e^{-j2k\tau_{o,n}N}} \cdot e^{j2k\tau_{o,n}\zeta} \tag{40}$$

where $\zeta = 2\sin(\phi/2)\sin(\phi'/2)$, and $N = \sqrt{\epsilon_r\mu_r - 1 + \zeta^2}$.

$$\begin{aligned} D^{sw}_{e,h}(\phi,\phi';\alpha_{sw}) = \mp\frac{e^{-j\pi/4}}{2\sqrt{2\pi k}} \\ \cdot \left[\frac{R^{swo}_{e,h}\left(\alpha^o_{sw},\phi'\right)}{\sin\left(\frac{\alpha^o_{sw} - \phi}{2}\right)}\left[1 - F_{KP}\left(kLa^o_{sw}\right)\right]\right. \\ + d^{swo}_{e,h}\left(\phi,\phi';\alpha^o_{sw}\right) + \frac{R^{swn}_{e,h}\left(\alpha^n_{sw},\phi'\right)}{\sin\left(\frac{\alpha^n_{sw} - \phi}{2}\right)} \\ \left. \cdot \left[1 - F_{KP}\left(kLa^n_{sw}\right)\right] + d^{swn}_{e,h}\left(\phi,\phi';\alpha^n_{sw}\right)\right], \end{aligned} \tag{41}$$

1944799x, 2007, 6, Downloaded from https://agupubs.onlinelibrary.wiley.com/doi/10.1029/2007RS003689, Wiley Online Library on [23/02/2023]. See the Terms and Conditions (https://onlinelibrary.wiley.com/terms-and-conditions) on Wiley Online Library for rules of use; OA articles are governed by the applicable Creative Commons License

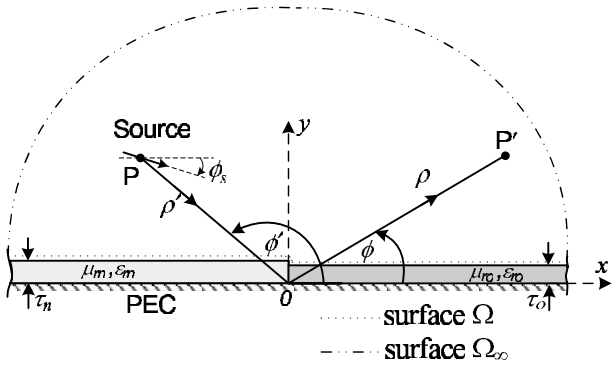

Figure 4. Line dipole source illumination of a junction between two different thin, planar DPS/DNG material slabs of different thickness on a PEC ground plane.

where $a^o_{sw} = 2\sin^2(\frac{\alpha^o_{sw}-\phi}{2})$, $a^n_{sw} = 2\sin^2(\frac{\alpha^n_{sw}-\phi}{2})$. Also

$$d^{swo}_{e,h}(\phi,\phi';\alpha^o_{sw}) = \frac{P^o_{e,h}(\alpha^o_{sw})}{Q^o_{e,h}(\phi)} \cdot \left[\sec\left(\frac{\alpha^o_{sw}-\phi'}{2}\right) \pm \sec\left(\frac{\alpha^o_{sw}+\phi'}{2}\right)\right]; \tag{42}$$

likewise, $d^{swn}_{e,h}(\phi,\phi';\alpha^n_{sw})$ can be found by replacing o by n in (42). The solution for the plane wave excitation case can be obtained by letting $\rho' \to \infty$ in the solution for the uniform line source illumination presented above.

2.3. Slope Diffraction Contribution

[29] When the source is a line dipole as shown in Figure 4, the dipole axis could be oriented to produce an incident field with a pattern null either in the direction of the discontinuity or close to it. In that case, the slope diffraction field dominates over the first-order UTD diffracted field. It is thus important to extend the UTD solution (given in section 2.2) to include a slope diffraction term. To do so, let the line dipole source be of the magnetic type at P' whose density is given by $\bar{M}_d = \hat{d}m_o\delta(x''-x')\delta(y''-y')$ with $\hat{d}\times\hat{z}=0$, and m_o is a known constant. Note also that $\hat{d}\cdot\hat{\rho}' = -\cos(\phi'+\phi_s)$ and $\hat{d}\cdot\hat{\phi}' = -\sin(\phi'+\phi_s)$. One may invoke the reciprocity theorem to find the electric field $\bar{E}$, which is produced by $\bar{M}_d$, and thus directly use the solution developed in section 2.2 to accomplish this task. Specifically, since the electric field $\bar{E}$ from a magnetic line dipole source $\bar{M}_d$ is entirely $\hat{z}$-directed, it can "react" with a $\hat{z}$-directed uniform electric line test source $\bar{J}' = \hat{z}I'_o\delta(x''-x)\delta(y''-y)$ at P, with I'_o being a known constant. The test source $\bar{J}'$ produces the fields $(\bar{E}', \bar{H}')$ where $\bar{E}' = \hat{z}E'$ can be obtained from section 2.2, i.e. $\bar{E}'(\rho,\phi) = \bar{E}^{i\prime} + \bar{E}^{s\prime}$, where $\bar{E}^{i\prime}$ and $\bar{E}^{s\prime}$ represent the $\hat{z}$-directed incident and scattered fields, respectively.

[30] Now, one can find $\bar{E}(\rho,\phi)$ from a knowledge of $\bar{E}'(\rho',\phi')$ via the reciprocity (or "reaction") theorem as:

$$\iint_\Omega \bar{E}\cdot\bar{J}'ds'' = -\iint_\Omega \bar{H}'\cdot\bar{M}_d ds'' \tag{43}$$

where $ds'' = dx''dy''$, and the closed region Ω is defined for $(|x| < \infty,\ 0 < y < \infty)$ as shown in Figure 4. Substituting for $\bar{J}'$ and $\bar{M}_d$ it then follows that $\bar{E}(\rho,\phi)\cdot\hat{z} = -m_o\frac{\hat{d}\cdot\bar{H}'}{I'_o}$. A UTD field description for $\bar{E}$ can be written symbolically as

$$\bar{E}(\rho,\phi) \sim \bar{E}^i + \bar{E}^r + \bar{E}^{sw} + \bar{\bar{E}}^d \tag{44}$$

where the superscripts have the same meaning as in section 2.2. The "tilde" on the field quantities on the RHS of (44) denote that the diffracted ($\tilde{E}^d$) terms, which includes both ordinary plus slope effects. One obtains the $\bar{E}^i$, $\bar{E}^r$, $\bar{E}^{sw}$, and $\bar{\bar{E}}^d$ after evaluating the CWS integral for $\bar{H}'$ on the RHS of (43) asymptotically. As indicated above $\bar{\bar{E}}^d$ contains a superposition of the first-order diffracted UTD space wave field originating from "0", and a slope diffracted UTD space wave field from "0", which can be expressed as

$$\tilde{E}^d_z(\rho,\phi) = \left[E^i_z(0)\left\{D^{go}_e(\phi',\phi) + D^{sw}_e(\phi',\phi;\alpha_{sw})\right\} + \frac{1}{jk\rho'}\frac{\partial}{\partial\phi'}E^i_z(0)\left\{D^{sd}_e(\phi',\phi) + D^{swd}_e(\phi',\phi;\alpha_{sw})\right\}\right]\cdot\frac{e^{-jk\rho}}{\sqrt{\rho}} \tag{45}$$

where $E^i_z(0)$ denotes the incident field at "0", which is given by $-\frac{k}{4}\frac{\sqrt{2j}}{\pi k}m_o\sin(\phi'+\phi_s)\frac{e^{-jk\rho'}}{\sqrt{\rho'}}$. In (45), the D^{go}_e and D^{sw}_e terms are the ordinary UTD contribution for the ray diffracted into space from "0" as discussed previously in (39) and (41), while the D^{sd}_e and D^{swd}_e refer to the slope effects (in the UTD ray context). In particular

$$D^{sd}_e(\phi',\phi) = -\frac{e^{-j\pi/4}}{4\sqrt{2\pi k}}\left\{\mathcal{R}^o_e(\phi) - \mathcal{R}^n_e(\phi)\right\} \cdot \left\{\frac{\sin\left(\frac{\phi'-\phi}{2}\right)}{\cos^2\left(\frac{\phi'-\phi}{2}\right)}F^s_{KP}\left(kLa^-_{go}\right) + \frac{\sin\left(\frac{\phi'+\phi}{2}\right)}{\cos^2\left(\frac{\phi'+\phi}{2}\right)}F^s_{KP}\left(kLa^+_{go}\right)\right\}, \tag{46}$$

1944799x, 2007, 6, Downloaded from https://agupubs.onlinelibrary.wiley.com/doi/10.1029/2007RS003689, Wiley Online Library on [23/02/2023]. See the Terms and Conditions (https://onlinelibrary.wiley.com/terms-and-conditions) on Wiley Online Library for rules of use; OA articles are governed by the applicable Creative Commons License

with $F^s_{KP}(\chi) = 2j\chi[1 - F_{KP}(\chi)]$. Also, the $D^{swd}_e = D^{swdo}_e + D^{swdn}_e$ with

$$D^{swdo}_e(\phi', \phi; \alpha^o_{sw}) = \frac{e^{-j\pi/4}}{2\sqrt{2\pi k}} \left[\frac{R^{swdo}_e(\alpha^o_{sw}, \phi)}{\sin\left(\frac{\alpha^o_{sw} - \phi'}{2}\right)} \cdot \left[1 - F_{KP}\left(kLa^o_{sw}\right)\right] + d^{swdo}_e(\phi', \phi; \alpha^o_{sw}) \right] \tag{47}$$

where

$$R^{swdo}_e(\alpha^o_{sw}, \phi) = -\frac{P^o_e(\alpha^o_{sw})}{2\left[Q^o_e(\alpha^o_{sw})\right]^2} Q^{o'}_e(\alpha^o_{sw}) \cdot \left[\sec\left(\frac{\alpha^o_{sw} - \phi}{2}\right) + \sec\left(\frac{\alpha^o_{sw} + \phi}{2}\right)\right] \tag{48}$$

$$d^{swdo}_e(\phi', \phi; \alpha^o_{sw}) = -\frac{P^o_e(\alpha^o_{sw})}{\left[Q^o_e(\phi')\right]^2} Q^{o'}_e(\phi') \cdot \left[\sec\left(\frac{\alpha^o_{sw} - \phi}{2}\right) + \sec\left(\frac{\alpha^o_{sw} + \phi}{2}\right)\right]. \tag{49}$$

[31] Note that all of the terms corresponding to *n*-face are the same as for the *o*-face case with *o* replaced by *n*, and the (ϵ_{ro}, μ_{ro}) for the *o*-face replaced by its material values (ϵ_{rn}, μ_{rn}) for *n*-face.

[32] If the magnetic line dipole source $\bar{M}_d$ in the above analysis is replaced by an electric line dipole source $\bar{J}_d$, then instead of $\bar{M}_d$ which radiates $\bar{E} = \hat{z}E_z$, the $\bar{J}_d$ will produce a magnetic field $\bar{H} = \hat{z}H_z$, which is entirely $\hat{z}$ polarized. Hence, the test source in this case would have to be a $\hat{z}$-directed uniform magnetic line source of strength M'_o at P and the diffraction coefficients in (45) are now replaced by D^{go}_h, D^{sw}_h, D^{sd}_h, and D^{swd}_h, respectively. It is also important to note that the result obtained in (45) for the $\bar{M}_d$ case is equally applicable to the case of a uniform electric line source of strength I_o when it is located directly on the material. In the latter case the $\tilde{E}^d_z$ in (45) is now produced by the slope diffraction of E^i_z incident from I_o. This E^i_z vanishes on the surface; hence, $\frac{\partial}{\partial\phi'}E^i_z$ represents its slope which is non zero. Likewise, the result for the $\bar{J}_d$ case will be directly applicable to the case of a uniform magnetic line source of strength M_o when it moves on to the material surface.

2.4. Surface Wave Diffraction

[33] Expressions for the launching of conventional FSWs, and BSWs (on the material slabs of Figure 1) due to diffraction at "0" of the wave incident from an external line source or line dipole source are presented above in sections 2.2 and 2.3, respectively. However, if the line source (or line dipole source) is placed very close to or on the thin material slab in Figure 1, but far from "0", then the source can noticeably and directly excite a FSW/BSW on the material slab as indicated earlier in section 2.2. Such a FSW/BSW carries power directly from the source to the discontinuity at "0" from where it can be diffracted into space. This is particularly true for the DPS (or DNG) junctions. The latter interaction is simply reciprocal to the launching of an FSW/BSW on the slab by diffraction of the wave incident at "0" from the source which is off the slab surfaces at $y = 0$ in Figure 1. Hence, the diffraction of an FSW/BSW at "0" which launches a diffracted ray into space is found directly via reciprocity from the result given in sections 2.2 and 2.3, for the launching of an FSW/BSW along the material slab in Figure 1 due to the diffraction at "0" of a wave incident from the source. This problem is useful in the design of surface wave antennas with DPS/DNG media.

3. Results

[34] Figure 5a shows the total field for TM plane wave scattering by the material half plane on a PEC entire plane of Figure 1, while Figure 5b shows the corresponding result for the geometry of Figure 2 with the same material half plane without a PEC entire plane. The new UTD results for the magnetic line source case are employed here to obtain the numerical plots with the line source removed to infinity ($\rho' \to \infty$) to simulate a TM plane wave illumination in the vicinity of the discontinuity at "0". The material thickness and electrical parameters are shown in the figures indicating that it is a thin negative (or DNG) material. The UTD based numerical plot of Figure 5a is compared in the same figure with a plot obtained from a corresponding W-H solution of *Rojas and Pathak* [1989] for the DPS half plane with a PEC entire plane after it is modified to remain valid for the DNG case. The approximate boundary conditions in the W-H solution become valid for the extremely thin half plane chosen here for the comparison. Likewise, the UTD plot in Figure 5b is compared with the W-H solution of *Volakis* [1988] which is also modified so that it becomes applicable to the DNG case. The UTD and W-H plots agree extremely well and are almost indistinguishable from each other for all cases in Figure 5. Figure 6 shows the pattern of a magnetic line dipole source placed tangentially on a DPS material strip

1944799x, 2007, 6, Downloaded from https://agupubs.onlinelibrary.wiley.com/doi/10.1029/2007RS003689, Wiley Online Library on [23/02/2023]. See the Terms and Conditions (https://onlinelibrary.wiley.com/terms-and-conditions) on Wiley Online Library for rules of use; OA articles are governed by the applicable Creative Commons License

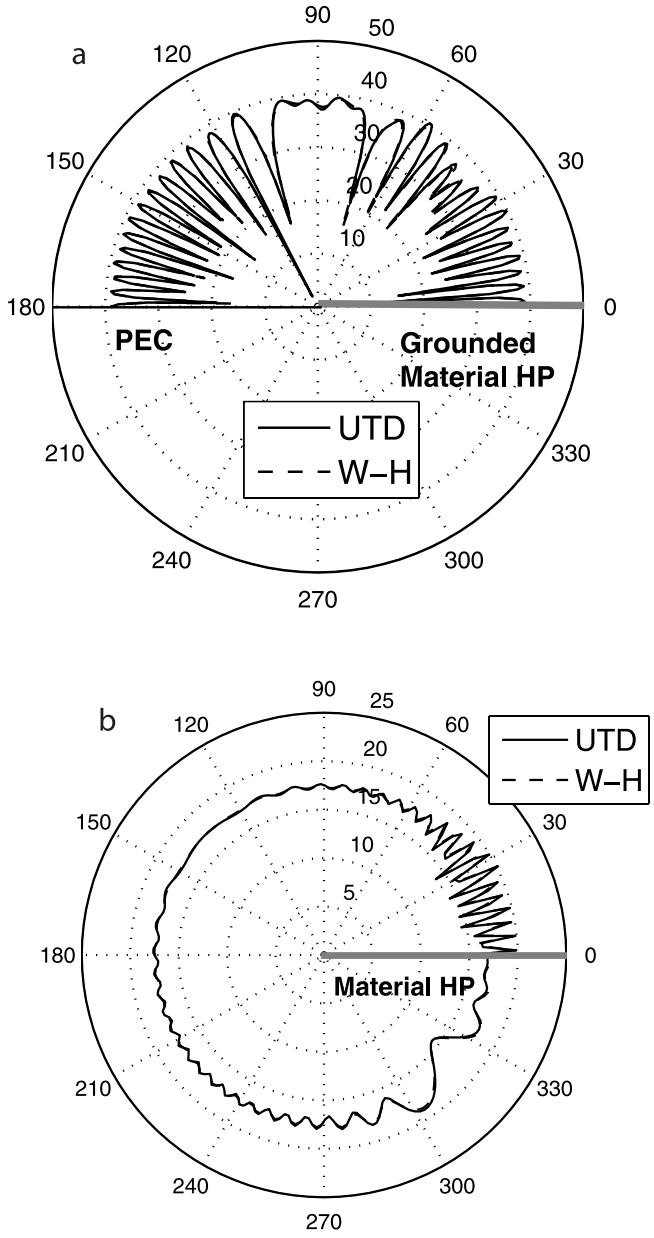

Figure 5. Comparison of UTD and W-H solutions for total magnetic fields at $\rho = 10\lambda$ from (a) two-part DNG material plane and (b) DNG material half plane. The material is $\lambda/20$ thick with $\epsilon_r = -2$ and $\mu_r = -3$. The illumination is a TM plane wave incident at $\phi' = 135°$.

1944799x, 2007, 6, Downloaded from https://agupubs.onlinelibrary.wiley.com/doi/10.1029/2007RS003689, Wiley Online Library on [23/02/2023]. See the Terms and Conditions (https://onlinelibrary.wiley.com/terms-and-conditions) on Wiley Online Library for rules of use; OA articles are governed by the applicable Creative Commons License

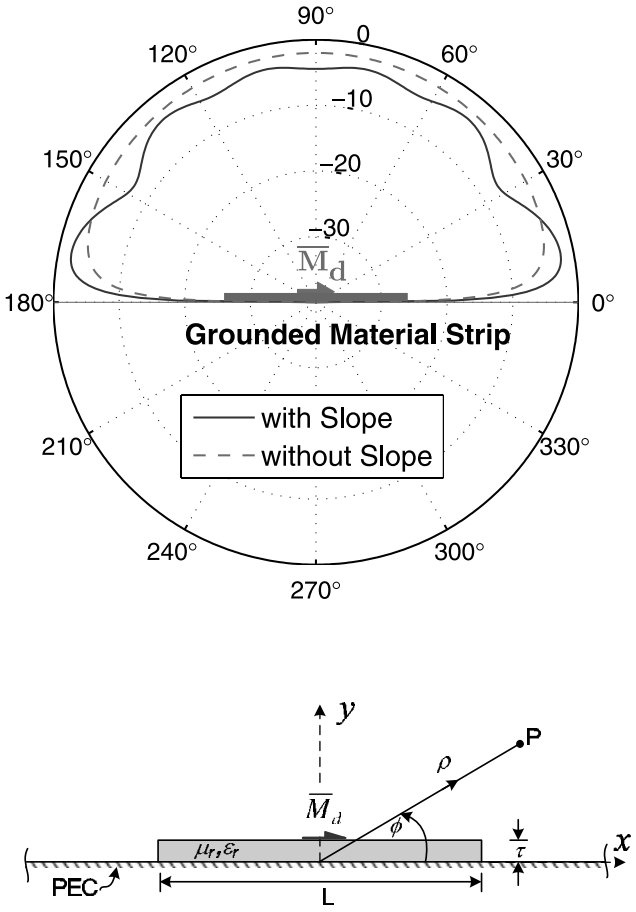

Figure 6. Effect of slope diffraction on the magnitude of total TE fields at $\rho = 100\lambda$ for a 5λ long material strip on a PEC entire plane. Strip has $\epsilon_r = 3.4$ and $\mu_r = 10$ with thickness $\lambda/20$. The excitation is a tangential ($\phi_s = 0°$) magnetic line dipole source located on the center of the strip.

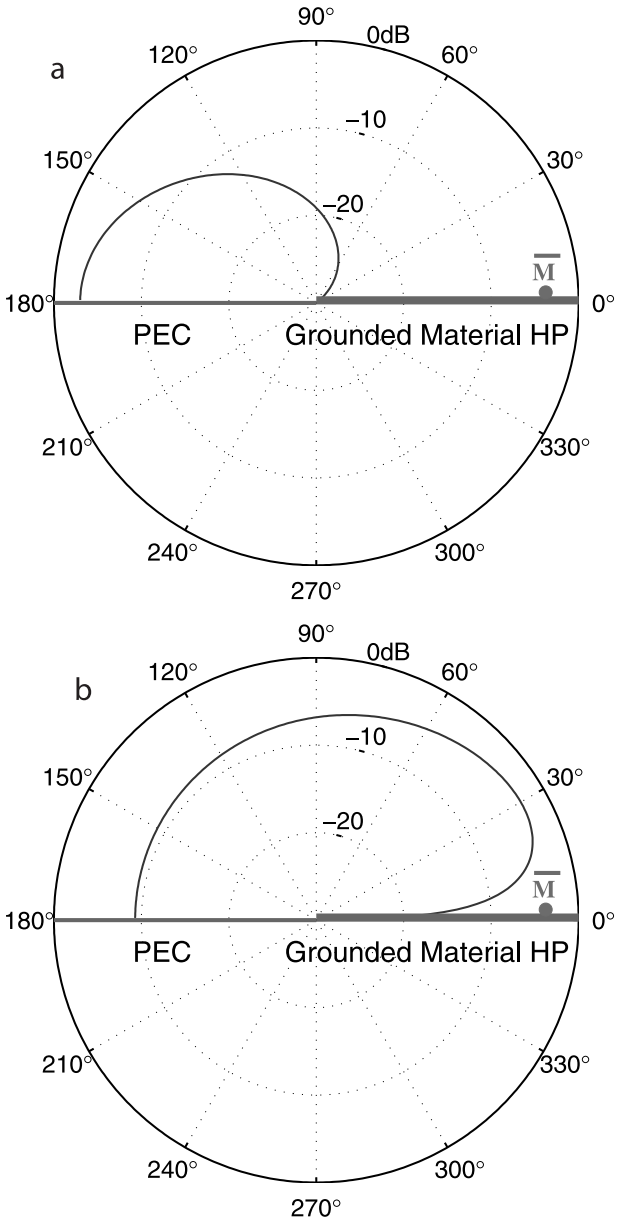

Figure 7. Only the Forward (Backward) surface wave diffracted field component of the total field is shown for an antenna (unit magnetic line source) at $\rho' = 5\lambda$, and $\phi' = 0°$ on a positive (negative) material half plane of thickness $\lambda/20$ over PEC entire plane. (a) FSW diffraction from a DPS half plane with $\epsilon_r = 2$ and $\mu_r = 3$. (b) BSW diffraction from a DNG half plane with $\epsilon_r = -18$ and $\mu_r = -19$.

of finite size on a PEC entire plane. This case is interesting because there is no SW excited by this type of source for the chosen thickness of the strip. Hence, the UTD slope diffraction effects become important because the first-order UTD field diffracted from both edges vanishes in this case. If the slope diffraction effects were not included, then only the pattern directly radiated by the source remains as would be true only if the strip edges were absent! Figure 7 illustrates the patterns of a surface wave antenna (or magnetic line source here) on a material half plane placed directly over a PEC entire plane as a special case of the geometry in Figure 1. In Figure 7a, the material is positive (DPS) and its thickness and electric properties are indicated in the

1944799x, 2007, 6, Downloaded from https://agupubs.onlinelibrary.wiley.com/doi/10.1029/2007RS003689, Wiley Online Library on [23/02/2023]. See the Terms and Conditions (https://onlinelibrary.wiley.com/terms-and-conditions) on Wiley Online Library for rules of use; OA articles are governed by the applicable Creative Commons License

figure; in contrast, the material is negative (DNG) for the case in Figure 7b. It is noted that the source excites a FSW in the case of Figure 7a, while in the case of Figure 7b it excites a BSW. The BSW diffraction in the DNG case produces an antenna pattern which is markedly different from the FSW diffraction for the DPS case.

4. Conclusions

[35] Accurate closed form asymptotic high frequency solutions are presented in the UTD format for the canonical problems of diffraction by thin planar positive (or negative) material structures with a discontinuity. These solutions can deal with different kinds of incident fields such as a plane wave, a cylindrical wave corresponding to a line/line dipole source excitation, and a forward (or backward) surface wave. They can be used to describe the radiation by (and coupling between) antennas near or on the material. The latter requires one to include higher UTD slope diffraction terms which are developed here in addition to the UTD fields diffracted to first order. Almost all previous related solutions do not contain slope diffraction effects because they deal with only uniform plane wave illumination. The latter solutions are typically based on W-H or Maliuzhinets methods, respectively, and use approximate impedance type boundary conditions. In contrast, the present asymptotic solutions of the wave equation, which are developed here via a heuristic spectral synthesis approach, provide UTD diffracted fields which satisfy reciprocity and the PEC boundary conditions as well as the Karp-Karal lemma. These UTD solutions also recover the proper FRTCs and the exact surface wave propagation constants, whereas the W-H or Maliuzhinets based solutions do not; consequently, the present solutions may be applicable to slightly thicker materials than is possible by the latter methods. Interesting radiation properties are observed for BSW antennas associated with negative (DNG) materials.

[36] Finally, a bisection method, described by *Rojas and Pathak* [1989], can be employed to directly synthesize a CWS for the problem in Figure 2 in terms of the CWS for the problem in Figure 1. This will be reported in a separate paper.

[37] **Acknowledgments.** The authors thank the reviewers for their helpful suggestions.

References

Burnside, W. D., and K. W. Burgener (1983), High frequency scattering by a thin lossless dielectric slab, *IEEE Trans. Antennas Propag.*, *AP-31*, 104–110.

Engheta, N., and R. W. Ziolkowski (2005), A positive future for double-negative metamaterials, *IEEE Trans. Microwave Theory Tech.*, *53*, 1535–1555.

Felsen, L. B., and N. Marcuvitz (1994), *Radiation and Scattering of Waves*, IEEE Press, Piscataway, N. J.

Kouyoumjian, R. G., and P. H. Pathak (1974), A Uniform Geometrical Theory of Diffraction for an edge in a perfectly conducting surface, *Proc. IEEE*, *62*, 1448–1461.

Luebbers, R. J. (1989), A heuristic UTD slope diffraction coefficient for rough lossy wedges, *IEEE Trans. Antennas Propag.*, *37*, 206–211.

Manara, G., R. Tiberio, G. Pelosi, and P. H. Pathak (1993), High-frequency scattering from a wedge with impedance faces illuminated by a line source, Part II: Surface wave, *IEEE Trans. Antennas Propag.*, *AP-41*, 877–883.

Nechayev, Y. I., and C. C. Constantinou (2006), Improved heuristic diffraction coefficients for an impedance wedge at normal incidence, *IEE Proc., Microwave Antennas Propag.*, *153*, 125–132.

Pathak, P. H. (1992), High frequency techniques for antenna analysis, *Proc. IEEE*, *80*, 44–65.

Pathak, P. H., and R. G. Kouyoumjian (1970), The dyadic diffraction coefficient for a perfectly conducting wedge, contract AF19 (628)-5929, Air Force Cambridge Res. Lab., Bedford, Mass.

Rojas, R. G., and P. H. Pathak (1989), Diffraction of EM waves by a dielectric/ferrite half-plane and related configurations, *IEEE Trans. Antennas Propag.*, *37*, 751–763.

Tiberio, R., G. Pelosi, G. Manara, and P. H. Pathak (1989), High-frequency scattering from a wedge with impedace faces illuminated by a line source, Part I: Diffraction, *IEEE Trans. Antennas Propag.*, *AP-37*, 212–218.

Volakis, J. L. (1988), High-frequency scattering by a thin material half plane and strip, *Radio Sci.*, *23*, 450–462.

Zucker, F. J. (1969), Surface-wave antennas, in *Antenna Theory*, vol. 2, edited by R. E. Collin and F. J. Zucker, pp. 298–348, McGraw-Hill, New York.

T. Lertwiriyaprapa, P. H. Pathak, and J. L. Volakis, ElectroScience Laboratory, Department of Electrical and Computer Engineering, 1320 Kinnear Road, Ohio State University, Columbus, OH 43212, USA. (lertwiriyaprapa.1@osu.edu; pathak.2@osu.edu; volakis.1@osu.edu)

1944799x, 2007, 6, Downloaded from https://agupubs.onlinelibrary.wiley.com/doi/10.1029/2007RS003689, Wiley Online Library on [23/02/2023]. See the Terms and Conditions (https://onlinelibrary.wiley.com/terms-and-conditions) on Wiley Online Library for rules of use; OA articles are governed by the applicable Creative Commons License